

UC Berkeley

UC Berkeley Previously Published Works

Title

Head to head comparison of [^{18}F] AV-1451 and [^{18}F] THK5351 for tau imaging in Alzheimer's disease and frontotemporal dementia.

Permalink

<https://escholarship.org/uc/item/60q0947p>

Journal

European journal of nuclear medicine and molecular imaging, 45(3)

ISSN

1619-7070

Authors

Jang, Young Kyoung
Lyoo, Chul Hyung
Park, Seongbeom
[et al.](#)

Publication Date

2018-03-01

DOI

10.1007/s00259-017-3876-0

Peer reviewed

Head to head comparison of [^{18}F] AV-1451 and [^{18}F] THK5351 for tau imaging in Alzheimer's disease and frontotemporal dementia

Young Kyoung Jang^{1,2} · Chul Hyoung Lyoo³ · Seongbeom Park¹ · Seung Jun Oh⁴ · Hanna Cho³ · Minyoung Oh⁴ · Young Hoon Ryu⁵ · Jae Yong Choi⁵ · Gil D. Rabinovici^{6,7} · Hee Jin Kim^{1,2} · Seung Hwan Moon⁸ · Hyemin Jang^{1,2} · Jin San Lee⁹ · William J. Jagust^{7,10} · Duk L. Na^{1,2,11} · Jae Seung Kim⁴ · Sang Won Seo^{1,2,11,12}

Received: 29 June 2017 / Accepted: 3 November 2017 / Published online: 16 November 2017
© Springer-Verlag GmbH Germany, part of Springer Nature 2017

Abstract

Purpose Tau accumulation is a core pathologic change in various neurodegenerative diseases including Alzheimer's disease and frontotemporal lobar degeneration-tau. Recently, tau positron emission tomography tracers such as [^{18}F] AV-1451 and [^{18}F] THK5351 have been developed to detect tau deposition in vivo. In the present study, we performed a head to head comparison of these two tracers in Alzheimer's disease and frontotemporal dementia cases and aimed to investigate which tracers are better suited to image tau in these disorders.

Methods A cross-sectional study was conducted using a hospital-based sample at a tertiary referral center. We recruited eight participants (two Alzheimer's disease, four frontotemporal dementia and two normal controls) who underwent magnetic resonance image, amyloid positron emission tomography with [^{18}F]-Florbetaben and tau positron emission tomography with both THK5351 and AV-1451. To measure regional AV1451 and THK5351 uptakes, we used the standardized uptake value ratios by dividing mean activity in target volume of interest by mean activity in the cerebellar hemispheric gray matter.

Electronic supplementary material The online version of this article (<https://doi.org/10.1007/s00259-017-3876-0>) contains supplementary material, which is available to authorized users.

✉ Jae Seung Kim
jaeskim@amc.seoul.kr

✉ Sang Won Seo
sangwonseo@empal.com

¹ Department of Neurology, Samsung Medical Center, Sungkyunkwan University School of Medicine, 81 Irwon-ro, Kangnam-ku, Seoul 06351, South Korea

² Neuroscience Center, Samsung Medical Center, Seoul, South Korea

³ Department of Neurology, Gangnam Severance Hospital, Yonsei University College of Medicine, Seoul, South Korea

⁴ Department of Nuclear Medicine, Asan Medical Center, University of Ulsan College of Medicine, 88 Olympic-ro 43-gil, Songpa-gu, Seoul 138-736, South Korea

⁵ Department of Nuclear Medicine, Gangnam Severance Hospital, Yonsei University College of Medicine, Seoul, South Korea

⁶ Memory and Aging Center, University of California, San Francisco, San Francisco, CA, USA

⁷ Helen Wills Neuroscience Institute, University of California, Berkeley, Berkeley, CA, USA

⁸ Department of Nuclear Medicine, Samsung Medical Center, Sungkyunkwan University School of Medicine, Seoul, South Korea

⁹ Department of Neurology, Kyung Hee University Hospital, Seoul, South Korea

¹⁰ Center of Functional Imaging, Lawrence Berkeley National Laboratory, Berkeley, CA, USA

¹¹ Department of Health Sciences and Technology, SAIHST, Sungkyunkwan University, Seoul, South Korea

¹² Department of Clinical Research Design & Evaluation, SAIHST, Sungkyunkwan University, Seoul, South Korea

Results Although THK5351 and AV-1451 uptakes were highly correlated, cortical uptake of AV-1451 was more striking in Alzheimer's disease, while cortical uptake of THK5351 was more prominent in frontotemporal dementia. THK5351 showed higher off-target binding than AV-1451 in the white matter, midbrain, thalamus, and basal ganglia.

Conclusions AV-1451 is more sensitive and specific to Alzheimer's disease type tau and shows lower off-target binding, while THK5351 may mirror non-specific neurodegeneration.

Keywords Tau · Av-1451 · THK5351 · Alzheimer's disease · Frontotemporal dementia

Introduction

Alzheimer's disease (AD) is characterized by extracellular neuritic plaques composed of aggregated amyloid-beta ($A\beta$) and intracellular neurofibrillary tangles (NFT) consisting of paired helical filaments (PHF) of hyperphosphorylated aggregated tau [1]. Frontotemporal dementia represents a family of disorders associated with either underlying tau aggregates (FTLD-tau) including pathological subtypes Pick's disease, corticobasal degeneration (CBD) and progressive supranuclear palsy (PSP) or TAR DNA-binding protein of 43 kDa (TDP-43) aggregates. The behavioral variant of FTD (bvFTD) is associated with underlying FTLT-tau in ~50% of patients. The language variant non-fluent variant primary progressive aphasia (nfvPPA) is usually (~70%) associated with underlying tauopathy, while semantic variant PPA (svPPA) is associated with FTLT-TDP in the vast majority (~80% of cases) [2–4]. In FTLT-tau, tau aggregates appear ultrastructurally as straight, randomly coiled or twisted filaments, rather than PHF [5]. Also, FTLT-tau has three repeats (3R) or four repeats (4R): 3R in Pick's disease and 4R in CBD and PSP [6].

Along with rapid development of molecular imaging, a number of promising tau positron emission tomography (PET) tracers including [^{18}F] THK5351 (THK5351) and [^{18}F] AV-1451 (AV-1451) have been developed. THK5351 has a higher tau affinity than amyloid β [7] and shows increased cortical uptake in AD and FTD syndromes [8, 9]. AV-1451 has more than 25-fold selectivity for tau over amyloid β [10]. AV-1451 also showed correlation with Braak's NFT stage [11, 12], cognitive status, and cortical atrophy [13]. In previous studies, both THK5351 and AV-1451 showed off-target binding, thought to be unrelated to tau, in the midbrain and basal ganglia [14, 15]. More recent pathology studies raised the possibility that THK5351 and AV-1451 have distinct characteristics. That is, AV-1451 binds to strongly PHF-tau observed in AD or FTD patients with specific mutations in the MAPT gene, but binding to straight form tau observed in most of FTLT-tau is weak to absent [16,

17]. However, THK-5351, a quinolone-derivative agent, might bind to monoamine oxidase B (MAO-B) [18]. Specifically, a significant proportion of THK signal may reflect normal MAO-B activity in basal ganglia or MAO-B expression from reactive astrocytes due to neuroinflammation states [19].

To our knowledge, there have been no head to head comparison studies imaging the same patients with both THK5351 and AV-1451. Given each tracer has distinct characteristics, comparing different tracers in the same subjects might be helpful to select the more suitable tracer in AD and FTD with different tau aggregates. Also, direct comparison of off-target binding between THK5351 and AV-1451 is important, particularly when the goal is to image subcortical tau deposition in certain disorders.

In the present study, we performed a head to head comparison of THK5351 and AV-1451 in AD, FTD and normal controls (NC). We determined whether the degree and distribution of THK5351 and AV-1451 cortical uptake differed between AD and FTD. We also examined whether THK5351 and AV-1451 tracers exhibited different degrees and distribution of off-target binding.

Materials and methods

Participants

Eight participants underwent magnetic resonance image (MRI), $A\beta$ PET with [^{18}F] Florbetaben (FBB) [20] and tau PET using with both [^{18}F] THK5351 and [^{18}F] AV-1451. Clinical diagnosis was established using standard research criteria for AD [21] and FTD dementia syndrome [22, 23]. Cases 1 and 2 were clinically diagnosed with early onset AD and logopenic variant primary progressive aphasia (lvPPA), a language-variant of AD [23]. Cases 3–6 were clinically diagnosed with FTD syndromes, including svPPA, nfvPPA and bvFTD ($N = 2$) [22–24]. Cases 7 and 8 were CN defined by detailed neuropsychological and neuroimaging studies. None of the participants had large infarction, brain tumor, or other brain lesions.

This study was approved by the institutional review board of Samsung Medical Center, and written informed consent was obtained from all participants.

[^{18}F] THK5351 PET acquisition

We acquired [^{18}F] THK5351 PET using a Discovery STE PET/CT scanner (GE Healthcare, Milwaukee, WI, USA) at Samsung Medical Center. [^{18}F] THK5351 PET images were acquired for 20 min, starting at 50 min after the IV bolus injection of 185 ± 18.5 MBq of ^{18}F -THK5351. Before the PET scan, we applied a head holder to minimize head motion

and also acquired brain CT images for attenuation correction. Finally, using the ordered-subsets expectation maximization algorithm (iteration = 4 and subset = 16), three dimensional (3D) PET images were reconstructed in a $128 \times 128 \times 47$ matrix with a $2.0 \times 2.0 \times 3.27$ mm voxel size.

[¹⁸F] AV-1451 PET acquisition

We acquired tau PET using a Biograph mCT PET/CT scanner (Siemens Medical Solutions, Malvern, PA, USA) at Gangnam Severance Hospital. [¹⁸F] AV-1451 PET images were acquired for 20 min, starting at 80 min after the IV bolus injection of 275.2 ± 28.0 MBq of [¹⁸F]AV-1451. Before the PET scan, we applied a head holder to minimize head motion and also acquired brain CT images for attenuation correction. Finally, using the ordered-subsets expectation maximization algorithm (iteration = 6 and subset = 16), 3-dimensional (3D) PET images were reconstructed in a $256 \times 256 \times 223$ matrix with a $1.591 \times 1.591 \times 1$ mm voxel size.

[¹⁸F] Florbetaben PET acquisition

All participants underwent FBB PET using a Discovery STE PET/CT scanner (GE Medical Systems, Milwaukee, WI, USA) or a Biograph mCT PET/CT scanner (Siemens Medical Solutions, Malvern, PA, USA) in 3D scanning mode that examined 35 slices of 4.25-mm thickness spanning the entire brain. A CT scan was performed for attenuation correction at 60 min after the injection using a 16-slice helical CT (140 KeV, 80 mA; 3.75 mm section width). A 20-min emission PET scan with dynamic mode (consisting of 4×5 min frames) was performed 90 min after injection into an antecubital vein as a bolus of a mean dose of 381 MBq. PET images were assessed visually by in-person-trained experts. Specifically, interpreters checked a regional cortical tracer uptake in the frontal, lateral temporal, posterior cingulate/precuneus, and parietal regions. Presence of increased uptakes in any of the four brain regions were regarded as amyloid β positivity [25].

MRI acquisition

All participants underwent brain MRI including three-dimensional (3D) T1 images at Samsung Medical Center using a 3.0 T MRI scanner (Philips 3.0 T Achieva; Best, the Netherlands). The following parameters were used for the 3D T1 images: sagittal slice thickness, 1.0 mm, over contiguous slices with 50% overlap; TR of 9.9 ms; TE of 4.6 ms; flip angle of 8°; and matrix size of 240×240 pixels, reconstructed to 480×480 over a field of view of 240 mm.

Amyloid and tau PET imaging analyses

PET images were co-registered to individual's MRIs, which were normalized to a T1-weighted MRI template. Using these parameters, MRI co-registered PET images were spatially normalized to the MRI template. MRI images were also segmented into brain tissue types and white matter images were classified to different lobes using the ANIMAL + INSECT algorithm [26, 27]. The quantitative cortical regional values were measured by an automated volume of interest (VOI) analysis tool using the automated anatomical labeling atlas. SPM version 8 through Matlab 2014b (Mathworks, Natick, MA, USA) was used for this analysis. FreeSurfer software package version 5.1 (<http://surfer.nmr.mgh.harvard.edu/>) was used to delineate subcortical region of interest (ROI) masks.

To measure regional AV1451 and THK5351 uptakes, we used the standardized uptake value ratios (SUVR) by dividing mean activity in target VOI by mean activity in the cerebellar hemispheric gray matter. We selected 28 cortical VOIs based on AAL template: bilateral frontal (superior and middle frontal gyri, medial part of superior frontal gyrus, opercular part of inferior frontal gyrus, triangular part of inferior frontal gyrus, supplementary motor area, orbital part of superior, middle, and inferior orbital frontal gyri, rectus and olfactory cortex), posterior cingulate gyri, parietal (superior and inferior parietal, supramarginal and angular gyri, and precuneus), lateral temporal (superior, middle and inferior temporal gyri, and heschl gyri), and occipital (superior, middle, and inferior occipital gyri, cuneus, calcarine fissure, and lingual and fusiform gyri). White matter images were parcellated into 2 regions: left hemisphere, and right hemisphere. White matter outline was set to 5 mm inside into white matter from the original outline to avoid gray matter spillover. Off-target VOIs were created by combining FreeSurfer ROIs: bilateral midbrain, thalamus, and basal ganglia.

Statistical analysis

Pearson correlation was performed to assess correlation between AV-1451 and THK-5351 in VOIs.

Results

Demographics

Demographic and clinical characteristics of our participants are shown in Table 1. Our participants were divided into two groups of equal numbers in each disease group according to the order of PET scans. That is, one group (1 AD, 2 FTD, 1 NC) performed THK5351 PET followed by AV-1451 PET while the other group (1 AD, 2 FTD, 1 NC) underwent AV-1451 PET at first, then THK5351 PET were done. There were

Table 1 Clinical characteristics of participants

	Case							
	1	2	3	4	5	6	7	8
Clinical diagnosis	AD	lvPPA	svPPA	nvPPA	bvFTD	bvFTD	NC	NC
Onset age (years)	52	55	68	60	59	71	64	67
Sex	Male	Female	Male	Male	Male	Male	Female	Female
Education	6	14	12	3	6	15	15	12
Apolipoprotein E	3/3	3/3	3/3	3/3	3/3	3/3	3/3	3/3
Family history of dementia	none	none	none	none	none	none	none	none
Handedness	Right	Right	Right	Right	Right	Right	Right	Right
MMSE	18	25	20	21	19	25	30	30
Age at tau PET	53	58	71	61	61	73	66	68
Imaging order	THK5351 -> AV-1451	AV-1451-> THK5351	AV-1451-> THK5351	THK5351 -> AV-1451	THK5351 -> AV-1451	AV-1451-> THK5351	AV-1451-> THK5351	THK5351 -> AV-1451
Interval between two tracers	3 months	6 months	6 months	5 months	5 months	6 months	4 months	2 months
Amyloid PET results	Positive	Positive	Negative	Negative	Negative	Negative	Negative	Negative

AD Alzheimer's dementia, *lvPPA* logopenic variant primary progressive aphasia, *svPPA* semantic variant primary progressive aphasia, *nvPPA* nonfluent/agrammatic primary progressive aphasia, *bvFTD* behavioral variant frontotemporal dementia, *NC* normal control

no differences in mean interval time between two images (3.8 ± 1.5 and 4.2 ± 1.4 months, $p = 0.733$). AD cases (case 1 and case 2) were amyloid PET positive while NC and FTD cases were amyloid PET negative.

Visual inspection of AV-1451 and THK5351 bindings

On visual inspection, AD cases (cases 1 and 2) showed extensive cortical AV-1451 and THK5351 binding. However, AV-1451 binding appeared to be more prominent over the large regions of cortex, whereas medial temporal binding was higher with THK5351. In svPPA (case 3), THK5351 PET showed increased uptake in the anterior and inferior temporal regions while AV-1451 PET showed increased uptakes just in

the white matter of those regions (Fig. 1). In nvPPA (case 4), the increased uptake was mainly observed in the left frontal white matter for both THK5351 and AV-1451 PET. However, uptake with THK5351 seemed to be more prominent than with AV-1451 (Fig. 1). Two bvFTD patients (cases 5 and 6) showed increased THK5351 binding primarily in the right frontal and temporal regions, while increased AV-1451 bindings were observed just in the white matter of those regions (Fig. 1). Two NC showed increased THK5351 binding in the medial temporal regions while there were no regions showing increased AV-1451 (Fig. 1). THK5351 binding seemed to be more prominent in the white matter, basal ganglia, thalamus and midbrain than AV-1451 binding in all patients. SUVR in each area of all patients were arranged in supplementary data 1.

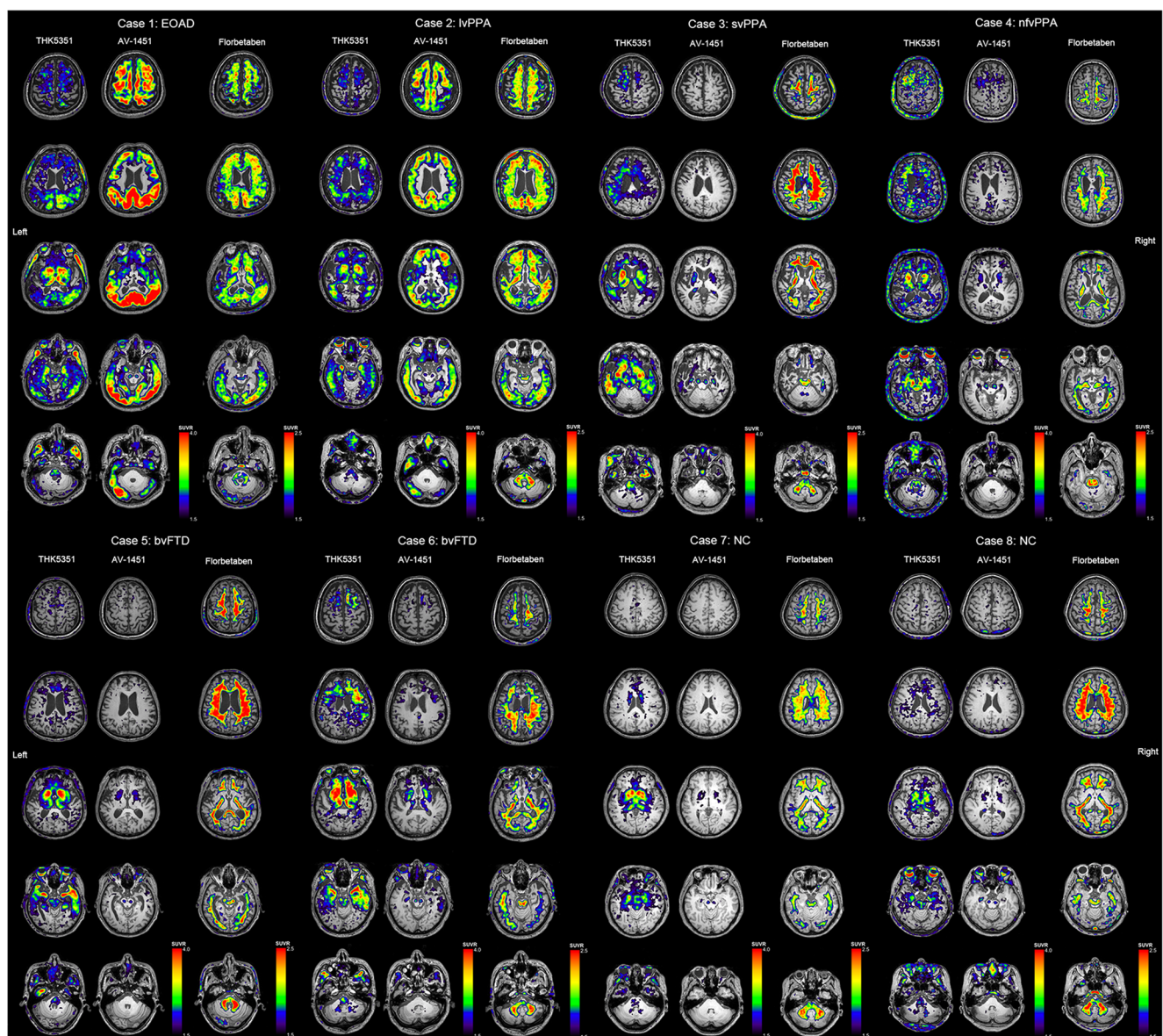


Fig. 1 THK5351 and AV-1451 uptake of participants. Patients with AD show higher and more extensive cortical uptake of AV-1451 than THK5351. In FTD, THK5351 shows higher retention than AV-1451. AD: Alzheimer's dementia; FTD: frontotemporal dementia

Correlation between AV-1451 and THK5351 uptakes

AV-1451 and THK5351 uptake was highly correlated in AD ($r = 0.63, p = 0.009$) and FTD ($r = 0.69, p < 0.001$) cases. Cortical AV1451 SUVR were higher than THK5351 SUVR in AD, whereas the opposite pattern was seen in FTD and controls (Fig. 2).

AD and FTD cases also showed high correlation ($|r| = 0.61$ to 0.99) between AV-1451 and THK5351 uptake in the white matter, midbrain, thalamus, and basal ganglia, with the exception of basal ganglia in AD cases (Fig. 3). In AD and FTD cases, THK5351 uptake was more prominent in the white matter, midbrain, thalamus, and basal ganglia with wider variations. However, AD cases showed that THK5351 and AV-1451 uptake had similar variation in the white matter while FTD cases showed THK5351 uptake had wider variation in the white matter than AV-1451 uptake.

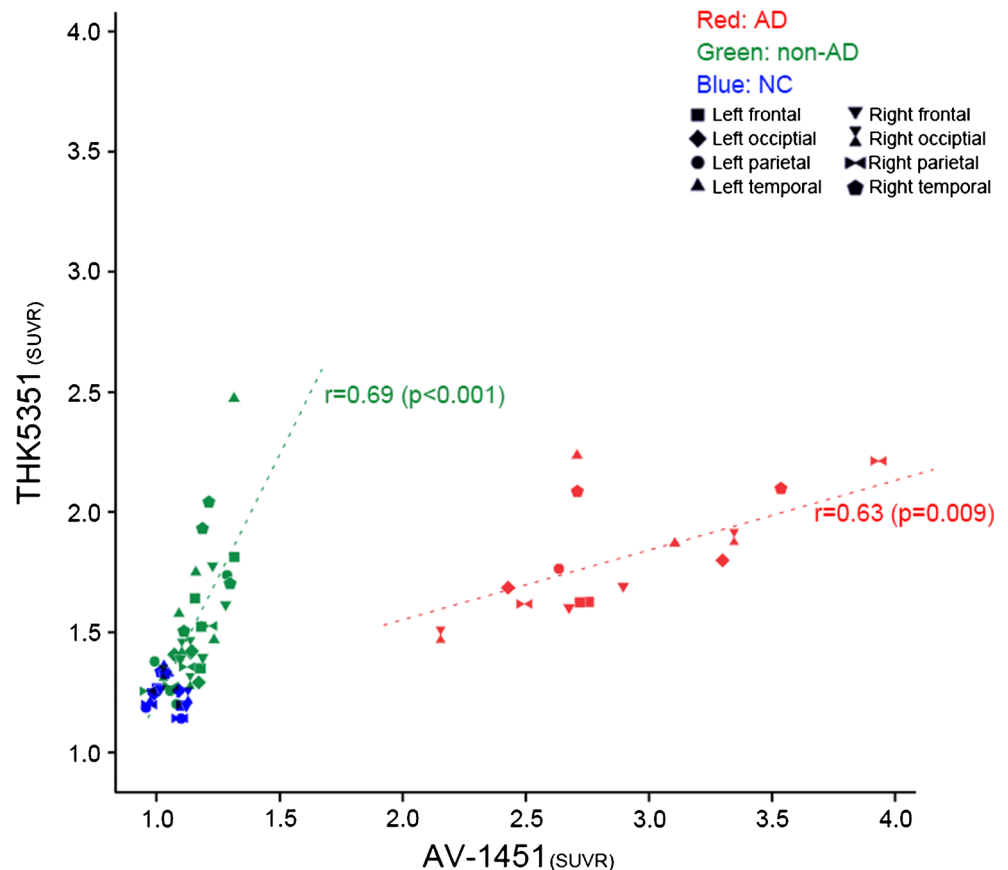
Discussion

In this study, we performed head to head comparisons of THK5351 and AV-1451 PET in patients clinically diagnosed with AD and FTD. We found that although THK5351 and AV-1451 tracers were highly correlated, cortical uptake of AV-

1451 was more striking in AD cases, while cortical uptake of THK5351 was more prominent in FTD and NC cases. Both THK5351 and AV-1451, regardless of type of dementia, showed off-target binding in the white matter, midbrain, thalamus, and basal ganglia, but THK5351 “off-target” binding was higher. Our preliminary results, therefore, suggest that AV-1451 is more sensitive and specific to AD type tau and less likely to present off-target binding, while THK5351 may mirror non-specific neurodegeneration.

Our first major finding was that AD cases showed higher cortical uptake of AV-1451 than THK5351. However, FTD cases showed higher cortical uptake of THK5351 than AV-1451. A previous study revealed that AV-1451 binding correlated with disease progression in the AD continuum [13] and also reflects Braak NFT staging [11]. However, other *in vivo* studies reported that AV-1451 binding seemed to be lower in FTD than in AD [13, 28]. Indeed, autoradiographic studies showed that AV-1451 had relatively selective binding to PHF-tau, the main form of aggregated tau in AD, than straight filaments of tau observed in Pick’s disease, CBD, or PSP [17, 29, 30]. Our findings therefore suggest that AV-1451 might have higher affinity to AD type NFT than other forms of tau, compared to THK5351. Interestingly, other groups have reported elevated AV1451 uptake in FTD patients with specific mutations in the *MAPT* gene that yield “AD-like” PHF-tau

Fig. 2 Correlation between THK5351 and AV-1451 uptake in cortical regions. AV-1451 and THK5351 uptake is highly correlated in AD and FTD cases. Cortical AV1451 SUVR are higher than THK5351 SUVR, whereas the opposite pattern is seen in FTD and controls. AD: Alzheimer’s dementia; FTD: frontotemporal dementia



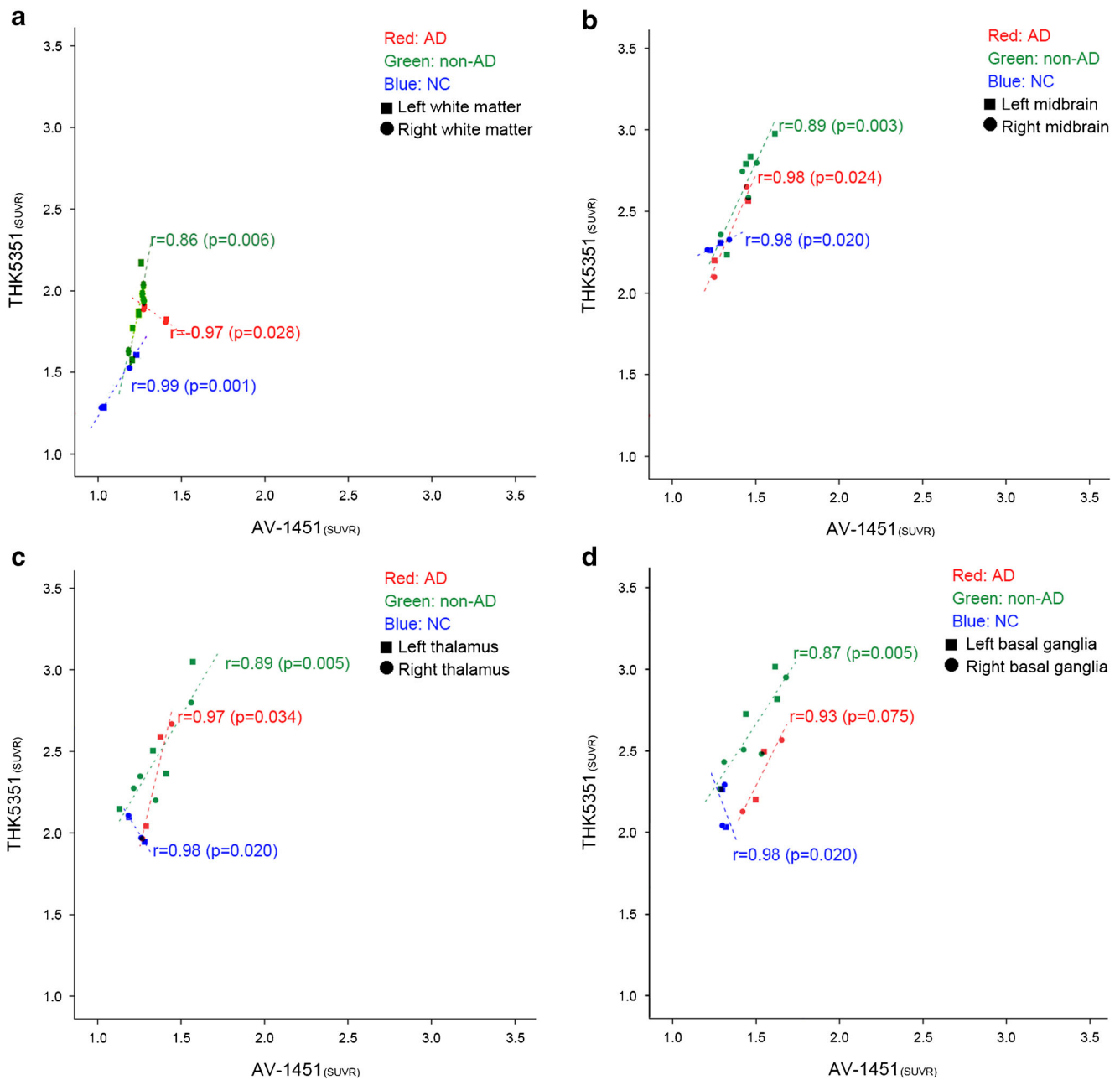


Fig. 3 Correlations between THK5351 and AV-1451 uptakes in (A) white matter, (B) midbrain, (C) thalamus, and (D) basal ganglia. AD and FTD cases show high correlation between AV-1451 and THK5351 uptake in the white matter, basal ganglia, thalamus and midbrain with the

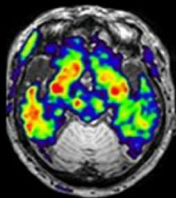
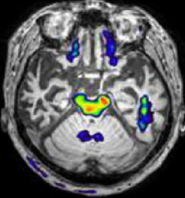
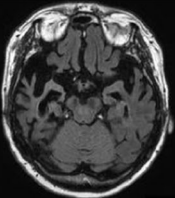
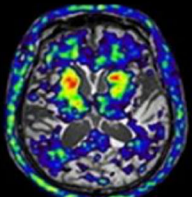
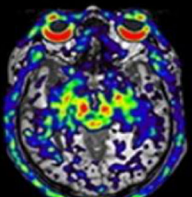
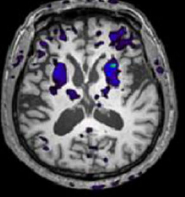
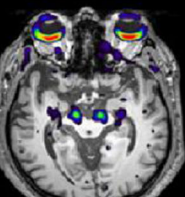
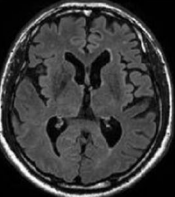
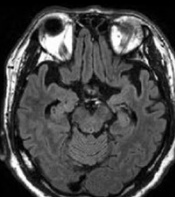
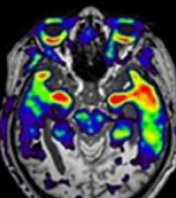
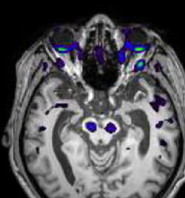
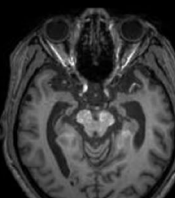
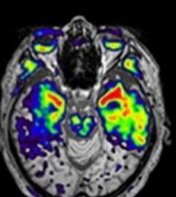
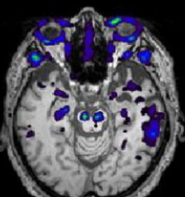
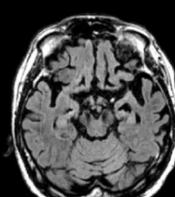
exception of white matter and basal ganglia in AD cases. THK5351 SUVR in these regions are higher than AV-1451 SUVR. AD: Alzheimer's dementia; FTD: frontotemporal dementia

aggregates that include a mix of 3R/4R isoforms, supporting the notion that this tracer shows a high-affinity for this specific type of tau aggregate [31, 32].

Previously, THK5351 binding in AD was reported primarily in temporoparietal, but not frontal regions, even in advanced AD dementia cases, compared to cognitively normal elderly [8, 14]. Patients with various FTD syndromes such as nfvPPA, svPPA, and bvFTD have been reported to show increased THK5351 uptake [33–35]. Consistent with previous reports, our findings, therefore, suggest that THK5351 is more

suitable for non-AD tauopathies compared to AV1451. Indeed, FTD syndrome showed that the topography of increased uptakes of THK5351 generally overlaps with brain atrophy on MRI and shows good correlation with clinical phenotypes while AV1451 showed increased uptakes just in white matter of atrophied regions on MRI (Table 2). Alternatively, THK5351 binding may target a non-specific process related to neurodegeneration that co-localizes with tau pathology. FTD syndromes consist heterogeneous patients with a variety of underlying neuropathologies. Furthermore,

Table 2 Clinical symptoms and imaging findings in the FTD cases

Case	Clinical diagnosis	Clinical symptoms	THK5351	AV-1451	MRI
3	Semantic variant PPA	Decreased understanding ability and confusion about names of objects without utterance problem.			
4	Nonfluent variant PPA	Laconic speech and difficulty in speaking what the patient thought.	 	 	 
5	Behavioral variant FTD	Prominent behavioral change without other cognitive impairment.			
6	Behavioral variant FTD	Apathetic mood and diminished social interest with sparing other cognitive function.			

FTD frontotemporal dementia, PPA primary progressive aphasia

~80% patients with clinical svPPA are found to have FTLDTDP rather than tau aggregates at autopsy [36, 37], but a previous study of THK5351 showed that six of six svPPA cases had increased uptakes in the anterior and inferior temporal regions [34]. Indeed, a more recent study suggested that THK5351 may indicate nonspecific neuronal injury rather than specific tauopathy [35]. A previous report also showed

that CJD patients had increased THK5351 uptake in cortical regions that also showed restricted diffusion on MRI [38]. Therefore, it might be related to MAO-B cross-reactivity. That is, THK-5351 might bind to increased MAO-B from reactive astrocytes in CJD [18, 39]. NC cases showed slight THK5351 uptakes in the cortical regions. Our findings were consistent with previous studies showing that normal elderly

had increased THK5351 uptakes in the cortical region. Considering that AV1451 showed increased uptake only in the choroid plexus, increased THK5351 uptakes in the cortical region might reflect MAO-B cross-reactivity [18]. In fact, in the post-selegiline scans, there was a significant uptake reduction in the cortical regions as well as striatum [19, 40]. However, one recent report revealed five svPPA patients showing increased AV-1451 uptake in the anterior temporal region [41]. In fact, when we lowered the cut-off value to SUVR 1.0, our svPPA patient also showed increased AV-1451 uptake in the anterior temporal region (supplementary data 2). It might be related to MAO-A cross-reactivity [42]. However, in the same scale (> SUVR 1.5) with THK5351, increased uptakes seemed to be more prominent in THK5351 than in AV-1451.

Our second major finding was that off-target regions such as the white matter, midbrain, thalamus, and basal ganglia showed more prominent uptake of THK5351 than was seen with AV-1451 with wider variation of uptake of THK5351 regardless of dementia types. Furthermore, even in NC, THK5351 binding seemed to be more prominent in these regions compared to AV-1451 binding. Therefore, our findings led us to postulate that different off-target patterns between THK5351 and AV-1451 binding might represent their binding affinities to different biomolecules. For example, increased THK5351 uptake in the basal ganglia and substantia nigra might reflect its binding to MAO-B [19]. Actually, even in normal controls, MAO-B expression increased in these regions [43]. Alternatively, increased AV-1451 uptake in these regions might reflect its binding to iron [30]. These regions are known to accumulate iron [44, 45]. In fact, a pathological study showed that AV-1451 might be associated with iron in these regions [30]. Also, it may be related to MAO-A. One previous study revealed that MAO-A inhibitor displaced the uptakes of AV1451 in normal brain tissue [42]. In conclusion, collectively, our findings suggested that AV-1451 is more sensitive and specific to Alzheimer disease type tau and shows lower off-target binding while THK5351 may reflect non-specific neurodegeneration.

The strength of our study is that we performed a head to head comparison of two tau tracers in the same subjects, allowing us to directly compare the characteristics of the two tracers in a variety of conditions. However, there are several limitations. First, we did not have pathological findings in these cases. Further studies with autopsy will be needed to confirm our findings. Second, there were an average of four months interval between AV-1451 and THK5351 scans. The prolonged delay in some cases leaves open the possibility that significant tau burden increased after the first scan and prior to the second scan. This argument is mitigated to some degree by no deviation of order to one ligand in the same syndromes. Finally, our number of cases is small, and our findings need to be replicated in larger samples. It is important to evaluate more

patients with pathologically or genetically confirmed or with syndromes which clinical diagnosis such as svPPA, PSP, FTD-ALS might be highly suggestive of pathologic diagnosis in the future study.

Funding This research was supported by a grant from the Korea Health Technology R&D Project through the Korea Health Industry Development Institute (KHIDI), funded by the Ministry of Health & Welfare, Republic of Korea (HI14C2768); and the National Research Foundation of Korea (NRF) grant funded by the Korea government (MSIP) (No. NRF-2017R1A2B2005081).

Compliance with ethical standards

Conflict of interest G.D.R. receives research support from Avid Radiopharmaceuticals, Eli Lilly, GE Healthcare and Piramal. He has received consulting fees and speaking honoraria from Eisai, Genentech, Roche, Lundbeck, Putnam and Merck.

Role of the funder The funders had no role in the design and conduct of the study; collection, management, analysis, and interpretation of the data; preparation, review, or approval of the manuscript; or decision to submit the manuscript for publication.

Ethical approval All procedures performed in studies involving human participants were in accordance with the ethical standards of the institutional and/or national research committee and with the 1964 Helsinki declaration and its later amendments or comparable ethical standards.

Informed consent Informed consent was obtained from all individual participants included in the study.

References

1. Trojanowski JQ, Clark CM, Schmidt ML, Arnold SE, Lee VM. Strategies for improving the postmortem neuropathological diagnosis of Alzheimer's disease. *Neurobiol Aging*. 1997;18:S75–9.
2. Mackenzie IR, Foti D, Woulfe J, Hurwitz TA. Atypical frontotemporal lobar degeneration with ubiquitin-positive, TDP-43-negative neuronal inclusions. *Brain*. 2008;131:1282–93.
3. Kertesz A, McMonagle P, Blair M, Davidson W, Munoz DG. The evolution and pathology of frontotemporal dementia. *Brain*. 2005;128:1996–2005.
4. Rascovsky K, Hodges J, Knopman D, Mendez M, Kramer J, Neuhaus J, et al. Can clinical features predict tau pathology in patients with behavioral variant frontotemporal dementia? Annual meeting of the American-Academy-of-Neurology. 2013.
5. Ariza M, Kolb HC, Moechars D, Rombouts F, Andres JJ. Tau positron emission tomography (PET) imaging: past, present, and future. *J Med Chem*. 2015;58:4365–82.
6. Dickson DW, Kouri N, Murray ME, Josephs KA. Neuropathology of frontotemporal lobar degeneration-tau (FTLD-tau). *J Mol Neurosci*. 2011;45:384–9.
7. Okamura N, Furumoto S, Harada R, Tago T, Yoshikawa T, Fodero-Tavoletti M, et al. Novel ¹⁸F-labeled arylquinoline derivatives for noninvasive imaging of tau pathology in Alzheimer disease. *J Nucl Med*. 2013;54:1420–7.
8. Okamura N, Furumoto S, Furukawa K, Ishiki A, Harada R, Iwata R, et al. PET imaging of tau pathology in mild cognitive impairment and Alzheimer's disease with [¹⁸F]THK-5351. Annual meeting of the Society-of-Nuclear-Medicine-and-Molecular-Imaging. 2015.

9. Ishiki A, Harada R, Okamura N, Tomita N, Rowe CC, Villemagne VL, et al. Tau imaging with [^{18}F]THK-5351 in progressive supranuclear palsy. *Eur J Neurol*. 2016.
10. Xia CF, Arteaga J, Chen G, Gangadharmath U, Gomez LF, Kasi D, et al. [^{18}F]T807, a novel tau positron emission tomography imaging agent for Alzheimer's disease. *Alzheimers Dement*. 2013;9:666–76.
11. Cho H, Choi JY, Hwang MS, Kim YJ, Lee HM, Lee HS, et al. In vivo cortical spreading pattern of tau and amyloid in the Alzheimer disease spectrum. *Ann Neurol*. 2016;80:247–58.
12. Chien DT, Bahri S, Szardenings AK, Walsh JC, Mu F, Su MY, et al. Early clinical PET imaging results with the novel PHF-tau radioligand [^{18}F]-T807. *J Alzheimers Dis*. 2013;34:457–68.
13. Cho H, Choi JY, Hwang MS, Lee JH, Kim YJ, Lee HM, et al. Tau PET in Alzheimer disease and mild cognitive impairment. *Neurology*. 2016;87:375–83.
14. Lockhart SN, Baker SL, Okamura N, Furukawa K, Ishiki A, Furumoto S, et al. Dynamic PET measures of tau accumulation in cognitively normal older adults and Alzheimer's disease patients measured using [^{18}F] THK-5351. *PLoS One*. 2016;11:e0158460.
15. Hansen AK, Knudsen K, Lillethorup TP, Landau AM, Parbo P, Fedorova T, et al. In vivo imaging of neuromelanin in Parkinson's disease using ^{18}F -AV-1451 PET. *Brain*. 2016;139:2039–49.
16. Marquie M, Normandin MD, Meltzer AC, Siao Tick Chong M, Andrea NV, Anton-Fernandez A, et al. Pathological correlations of [^{18}F]-AV-1451 imaging in non-alzheimer tauopathies. *Ann Neurol*. 2017;81:117–28.
17. Marquie M, Normandin MD, Vanderburg CR, Costantino IM, Bien EA, Rycyna LG, et al. Validating novel tau positron emission tomography tracer [^{18}F]-AV-1451 (T807) on postmortem brain tissue. *Ann Neurol*. 2015;78:787–800.
18. Lee MK, Hwang BY, Lee SA, Oh GJ, Choi WH, Hong SS, et al. 1-methyl-2-undecyl-4(1H)-quinolone as an irreversible and selective inhibitor of type B monoamine oxidase. *Chem Pharm Bull (Tokyo)*. 2003;51:409–11.
19. Ng KP, Massarweh G, Soucy JP, Gravel P, Pascoal TA, Mathotaarachchi S, et al. Selegiline reduces brain [^{18}F]THK5351 binding. 11th Human Amyloid Imaging. 2017;187.
20. Rowe CC, Ackerman U, Browne W, Mulligan R, Pike KL, O'Keefe G, et al. Imaging of amyloid beta in Alzheimer's disease with 18F-BAY94-9172, a novel PET tracer: proof of mechanism. *Lancet Neurol*. 2008;7:129–35.
21. McKhann GM, Knopman DS, Chertkow H, Hyman BT, Jack CR Jr, Kawas CH, et al. The diagnosis of dementia due to Alzheimer's disease: recommendations from the National Institute on Aging-Alzheimer's Association workgroups on diagnostic guidelines for Alzheimer's disease. *Alzheimers Dement*. 2011;7:263–9.
22. Rascovsky K, Hodges JR, Knopman D, Mendez MF, Kramer JH, Neuhaus J, et al. Sensitivity of revised diagnostic criteria for the behavioural variant of frontotemporal dementia. *Brain*. 2011;134:2456–77.
23. Gorno-Tempini ML, Hillis AE, Weintraub S, Kertesz A, Mendez M, Cappa SF, et al. Classification of primary progressive aphasia and its variants. *Neurology*. 2011;76:1006–14.
24. Neary D, Snowden JS, Gustafson L, Passant U, Stuss D, Black S, et al. Frontotemporal lobar degeneration: a consensus on clinical diagnostic criteria. *Neurology*. 1998;51:1546–54.
25. Barthel H, Luthardt J, Becker G, Patt M, Hammerstein E, Hartwig K, et al. Individualized quantification of brain beta-amyloid burden: results of a proof of mechanism phase 0 florbetaben PET trial in patients with Alzheimer's disease and healthy controls. *Eur J Nucl Med Mol Imaging*. 2011;38:1702–14.
26. Collins DL, Holmes CJ, Peters TM, Evans AC. Automatic 3-D model-based neuroanatomical segmentation. *Hum Brain Mapp*. 1995;3:190–208.
27. Collins DL, Zijdenbos AP, Baaré WFC, Evans AC. ANIMAL+INSECT: Improved cortical structure segmentation. In: Kuba A, Šámal M, Todd-Pokropek A, editors. Information processing in medical imaging: 16th international conference, IPMI'99 Visegrád, Hungary, June 28 – July 2, 1999 Proceedings. Berlin, Heidelberg: Springer Berlin Heidelberg; 1999. p. 210–23.
28. Martersteck A, Sridhar J, Rainford A, Mesulam M, Rogalski E. Recovering signal from AV1451 in frontotemporal lobar degeneration with partial volume correction. 11th Human Amyloid Imaging; 2017. p. 176.
29. Sander K, Lashley T, Gami P, Gendron T, Lythgoe MF, Rohrer JD, et al. Characterization of tau positron emission tomography tracer [^{18}F]AV-1451 binding to postmortem tissue in Alzheimer's disease, primary tauopathies, and other dementias. *Alzheimers Dement*. 2016;12:1116–24.
30. Lowe VJ, Curran G, Fang P, Liesinger AM, Josephs KA, Parisi JE, et al. An autoradiographic evaluation of AV-1451 tau PET in dementia. *Acta Neuropathol Commun*. 2016;4:58.
31. Smith R, Puschmann A, Scholl M, Ohlsson T, van Swieten J, Honer M, et al. ^{18}F -AV-1451 tau PET imaging correlates strongly with tau neuropathology in MAPT mutation carriers. *Brain*. 2016;139:2372–9.
32. Spina S, Schonhaut DR, Boeve BF, Seeley WW, Ossenkoppele R, O'Neil JP, et al. Frontotemporal dementia with the V337M MAPT mutation: tau-PET and pathology correlations. *Neurology*. 2017.
33. Hwang J, Kim JE, Park S-H, Roh JH, Lee J-H. A Non-fluent agrammatic primary progressive aphasia documented with an ^{18}F -THK5351-PET. 2016 Annual Spring Meeting of Korean Dementia Association; 2016.
34. Lee H, Lee S-Y, Jeong HJ, Woo S-H, Lee K-M, Lee Y-B, et al. Tau PET imaging in patients with semantic variant primary progressive aphasia 35th 2016 Annual Autumn Meeting of the Korean Neurological Association; 2016.
35. Kim JE, Hwang J, Park S-H, Oh M, Kim JS, Lee J-H, et al. ^{18}F -THK5351 PET findings indicative of brain injury rather than presumptive pathology in FTL D. 35th 2016 Annual Autumn Meeting of the Korean Neurological Association; 2016. p. 171.
36. Hodges JR, Mitchell J, Dawson K, Spillantini MG, Xuereb JH, McMonagle P, et al. Semantic dementia: demography, familial factors and survival in a consecutive series of 100 cases. *Brain*. 2010;133:300–6.
37. Snowden J, Neary D, Mann D. Frontotemporal lobar degeneration: clinical and pathological relationships. *Acta Neuropathol*. 2007;114:31–8.
38. Kim JE, Hwang J, Park S-H, Ko MA, Lee Y, Lee J-H, et al. Combined [^{18}F]Florbetaben Amyloid PET and [^{18}F]THK-5351 Tau PET as a potential pathfinder in a patient with rapidly progressive dementia. 2016 Annual Spring Meeting of the Korean Dementia Association; 2016. p. 165.
39. Kawamoto Y, Akiguchi I, Jarius C, Budka H. Enhanced expression of 14-3-3 proteins in reactive astrocytes in Creutzfeldt-Jakob disease brains. *Acta Neuropathol*. 2004;108:302–8.
40. Ng KP, Pascoal TA, Mathotaarachchi S, Theriault J, Kang MS, Shin M, et al. Monoamine oxidase B inhibitor, selegiline, reduces ^{18}F -THK5351 uptake in the human brain. *Alzheimers Res Ther*. 2017;9:25.
41. Bevan-Jones WR, Cope TE, Jones PS, Passamonti L, Hong YT, Fryer TD, et al. [^{18}F]AV-1451 binding in vivo mirrors the expected distribution of TDP-43 pathology in the semantic variant of primary progressive aphasia. *J Neurol Neurosurg Psychiatry*. 2017.
42. Hostetler ED, Walji AM, Zeng Z, Miller P, Bennacef I, Salinas C, et al. Preclinical characterization of ^{18}F -MK-6240, a promising PET

- tracer for in vivo quantification of human Neurofibrillary tangles. *J Nucl Med*. 2016;57:1599–606.
43. Fowler JS, Volkow ND, Wang GJ, Logan J, Pappas N, Shea C, et al. Age-related increases in brain monoamine oxidase B in living healthy human subjects. *Neurobiol Aging*. 1997;18:431–5.
44. Aquino D, Bizzi A, Grisoli M, Garavaglia B, Bruzzone MG, Nardocci N, et al. Age-related iron deposition in the basal ganglia: quantitative analysis in healthy subjects. *Radiology*. 2009;252:165–72.
45. Massey LA, Miranda MA, Al-Helli O, Parkes HG, Thomson JS, So PW, et al. 9.4 T MR microscopy of the substantia nigra with pathological validation in controls and disease. *Neuroimage Clin*. 2017;13:154–63.